surfaces and, in the dark reaction, eventually returns to the ground-state surface.

In the dark reaction, the flux that reaches the $^2A'$ surface must evolve to either ground-state products or ground-state reagents because there is not enough energy to form an asymptotic excited state (*10*). No information is yet available about the relative proportions of reagents or products formed from the flux leaving the 2A′ surface, although the reagents might be reformed by a reversal of the initial hop. Perhaps some evidence that this reversal is taking place is that experimental reactive branching fractions for similar systems tend to be lower than statistical estimates, suggesting that some of the flux could be diverted to a nonreactive surface (*11*). However, these measurements of branching fractions are a blunt probe of the fate of the 2A′ flux because they are dominated by the contributions of paths restricted to the ground-state surface.

We thus believe that this reaction normally occurs through two complementary pathways. One path is confined to the ground-state electronic surface, and the second is a path that includes a hop onto an excited electronic surface for several molecular vibrations and then a return to the ground surface. Normal "state-to-state" methods of chemical dynamics, which only probe the asymptotic states of either the reagents or products, are unlikely to yield evidence of this behavior. The current approach, which directly probes the intermediates of the reaction by transition species spectroscopy, offers direct evidence for a transient population of an excited state in a ground-state chemical reaction. One might describe the system as "stopping off for a beer" on the way to reaction; it may or may not lose its way after leaving the bar.

REFERENCES AND NOTES

1. For reviews, see P. R. Brooks, *Chem. Rev.* **88**, 407 (1988); A. H. Zewail, *Faraday Discuss. Chem. Soc.* **91**, 207 (1991); D. M. Neumark, *Annu. Rev. Phys. Chem.* **43**, 153 (1992).
2. P. Arrowsmith, S. H. P. Bly, P. E. Charters, P. Chevrier, J. C. Polanyi, *J. Phys. Chem.* **93**, 4716 (1989); J. S. Keller, P. W. Kash, E. Jensen, L. J. Butler, *J. Chem. Phys.* **96**, 4324 (1992); A. G. Suits, H. Hou, H. F. Davis, Y. T. Lee, J.-M. Mestdagh, *ibid.* **95**, 8178 (1991). The theoretical study of an excited-state reaction $O(^1D) + H_2$ suggests behavior similar to that proposed here [P. A. Berg, J. J. Sloan, P. J. Kuntz, *ibid.*, p. 8038].
3. P. R. Brooks, R. F. Curl, T. C. Maguire, *Ber. Bunsenges. Phys. Chem.* **86**, 401 (1982).
4. M. D. Barnes, P. R. Brooks, R. F. Curl, P. W. Harland, *J. Chem. Phys.* **94**, 5245 (1991); *ibid.* **96**, 3559 (1992); T. C. Maguire, P. R. Brooks, R. F. Curl, J. H. Spence, S. J. Ulvick, *ibid.* **85**, 844 (1986).
5. Large cross sections for changing the fine structure states of sodium are well known [L. Krause, *Adv. Chem. Phys.* **28**, 267 (1975)] and the states might be expected to be scrambled. However, highly nonstatistical fine structure state distributions can result from the photodissociation of alkali dimers [J. X. Wang, P. D. Kleiber, K. M. Sando, W. C. Stwalley, *Phys. Rev. A* **42**, 5352 (1990); E. W. Rothe, U. Krause, R. Düren, *J. Chem. Phys.* **72**, 5145 (1980)].
6. K. Yamashita and K. Morokuma, *J. Phys. Chem.* **92**, 3109 (1988); *J. Chem. Phys.* **91**, 7477 (1989).
7. K. I. Peterson, P. D. Dao, A. W. Castleman, *J. Chem. Phys.* **79**, 777 (1983); M. M. Kappes, P. Radi, M. Schaer, E. Schumacher, *Chem. Phys. Lett.* **113**, 243 (1985).
8. M. C. Moulton, and D. R. Herschbach, *J. Chem. Phys.* **44**, 3010 (1967); S. K. Neoh and D. R. Herschbach, *ibid.* **63**, 1030 (1975).
9. The excitation of trapped flux in diatomic systems has been directly observed in the femtosecond dynamics of the photodissociation of NaX [T. S. Rose, M. J. Rosker, A. H. Zewail, *ibid.* **91**, 7415 (1989)].
10. Laser excitation can, of course, supply the necessary energy for the formation of excited product Na*.
11. S. A. Safron, thesis, Harvard University (1969); S. Stolte, A. E. Proctor, R. B. Bernstein, *J. Chem. Phys.* **65**, 4990 (1976).

12. Supported by the Robert A. Welch Foundation and National Science Foundation grant CHE 87-19403.

16 April 1993; accepted 2 July 1993

Why Silicon Is Hard

John J. Gilman

Compared with pure metals and ionic salts, covalent solids such as silicon are hard and brittle because dislocations do not move in them except at high temperatures. A satisfactory explanation for this behavior has been lacking in spite of its great importance for the mechanics of materials and structures. It is shown here that the critical atomic process leading to the observed brittleness is analogous to a chemical substitution reaction. Analysis of this analogy with the aid of a correlation diagram yields the observed high resistive stress and high activation energy. When a kink on a dislocation line moves, it breaks the atomic bonding symmetry, a forbidden process.

Pure metals are often quite soft (even at very low temperatures), whereas covalent solids such as silicon are hard and brittle at all temperatures below their Debye temperatures. This difference in behavior has not been properly explained by current theories of dislocations. The standard Peierls-Nabarro theory gives the stress needed for a dislocation line to overcome the maximum crystal potential (with the assistance of thermal activation) (*1*). The equation it gives for this stress has the form: $3G[\exp(-10a/b)]$, where G is the shear modulus, a is the glide plane spacing, and b is the Burgers displacement. For the diamond structure, $a/b \simeq 1.8$ and so the stress is about 10^{-3} G, which is two orders of magnitude smaller than observations. Furthermore, metals such as copper and aluminum have nearly the same shear moduli as silicon but are three orders of magnitude softer at the same purity level.

The technical difficulties of the Peierls-Nabarro theory have been discussed by Nabarro (*1*) and by Hirth and Lothe (*2*). Its general deficiency is that it is a classical theory, so it should not be expected to be applicable at the atomic scale of chemical bonds. The fundamental nature of a dislocation's motion is that of a chemical substitution reaction of the type described by Woodward and Hoffmann (*3*) as a disconcerted process (that is, a forbidden one). The motion of a dislocation can be analyzed in a simple way by means of a Walsh correlation diagram.

Lawrence Berkeley Laboratory, Berkeley, CA 94720.

Dislocation lines do not move concertedly; rather, they move through kinks that lie along their lengths. If the average kink velocity along a line is v_k and the kink concentration is c_k, then the dislocation line velocity v_d is given by $\alpha c_k v_k$, where α is a geometric factor of order unity. The conventional theory is based on the idea that the rate-determining step is the rate of formation of kink pairs and that kink mobilities are high (*4*). However, this theory is quite tenuous for both theoretical (*1*, *2*) and experimental reasons. Direct measurements of kink formation rates have not been possible, and theoretical estimates are not reliable. Also, the behavior of crystals is inconsistent with the model. According to kink nucleation theory, if a crystal were flowing plastically at a high temperature and the temperature were quickly decreased, there should be a transient period during which the crystal would continue to flow. This is not observed. The activation energies that are observed for dislocation motion are sharply defined and independent of the applied stress (*4*, *5*). If kink pair formation were controlling the rate, there should be a spectrum of activation energies. Furthermore, at low stress levels the activation length for kink pair formation is too large for a dominant thermal activation process because the phonon wavelengths are short and their phases are random above the Debye temperature. Therefore, the probability of reaching the activated transition state is very small. Consequently, kink mobility must control the overall rate.

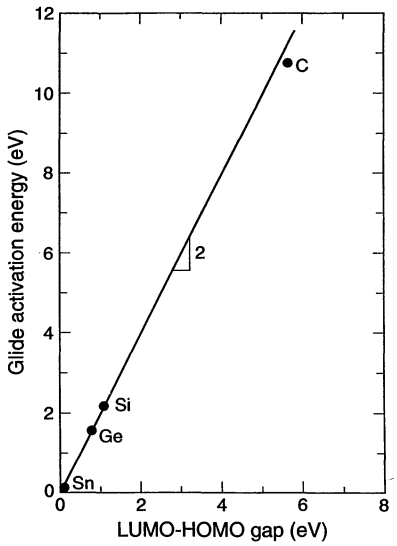

Fig. 1. Proportionality between the observed activation energy for dislocation motion in homopolar covalent crystals and their LUMO-HOMO energy gaps.

In the conventional theory, the difficulties cited above are extracted into the preexponential factor of the rate equation and then ignored. In the open diamond structure of silicon, for example, kinks can be very localized in accordance with the observed strong temperature dependence of the measured rates. Localized kinks are also consistent with the well-defined activation energy and its independence of the applied stress. They are also consistent with the highly directional bonds found in covalent crystals and with the fact that the bonding electrons are spin-paired. Similarly, the fact that the dislocation velocity is linearly proportional to the applied stress means that there is efficient momentum transfer across the glide planes during the motion.

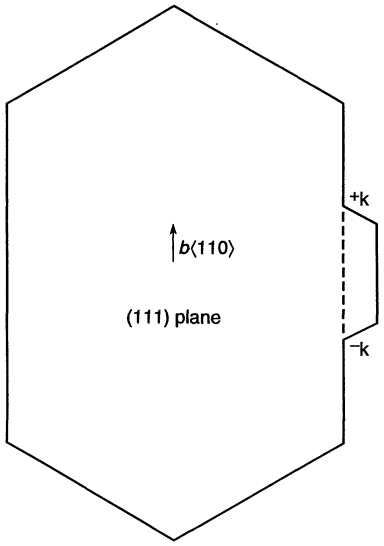

Fig. 2. Schematic dislocation loop with a kink pair lying on the (111) plane of a crystal with the diamond structure; b is the Burgers vector.

Fig. 3. Arrangement of chemical bonds at the center of a kink in a homopolar diamond-structure crystal. The cross-hatched ellipses represent the sp^3 bonding orbitals. The dislocation line approaches the plane of the figure from the front right (at 60°) and recedes from the plane of the figure from the back left. Note the loss of overlap of the bonding orbitals at the very center of the drawing.

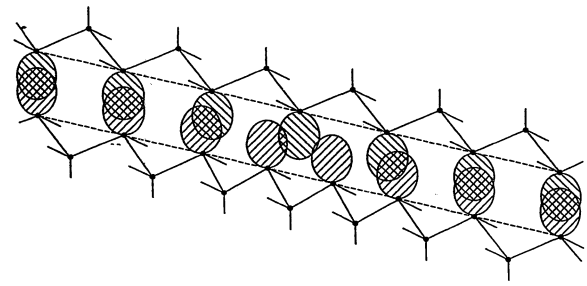

It has been observed that the activation energy for dislocation motion equals twice the HOMO-LUMO energy gap (6) [HOMO is the highest occupied molecular orbital; LUMO is the lowest unoccupied molecular orbital (Fig. 1)]. For homopolar semiconductors (carbon, silicon, germanium, and tin) the HOMO level equals the top of the valence band, and the LUMO level equals the bottom of the conduction band. This suggests that the kink mobility is directly related to the electronic structure rather than being indirectly related through elastic stiffnesses.

Consider the pertinent local kink geometry. Figure 2 is a sketch of a dislocation loop lying on a (111) plane of the diamond structure. Measurements show that the screw orientations move most slowly under a given stress so kinks on them are rate-determining. A schematic pair of these is shown. The chemical structure of one kink at the atomic level is shown in Fig. 3. The kink is part of a dislocation line that comes out of the plane of the drawing on the right side (at 60°), jogs at the kink, and then extends out of the back of the plane of the drawing on the left side (at 60°). Thus, the region is asymmetric. Furthermore, the space surrounding the kink is multiply connected, so circuits taken around the dislocation line (normal to the plane of the drawing) undergo a phase shift of b each time a circuit of 2π is completed.

The cross-hatched ellipses in Fig. 3 represent sp^3 hybrid orbitals. Four bonds surround each atom, pointing toward the corners of a tetrahedron. In each case only one of them consists of a pair of schematic orbitals; the others are represented as sticks.

Bonds form where the sp^3 orbitals overlap (indicated by double crosshatching in Fig. 3). The bonds are quite resistant to shear distortions (bending), as discussed by Phillips (7). If they were not, the structure would collapse to some close-packed configuration.

The "horizontal" plane of Fig. 3 is a (111) plane of the diamond structure, and the direction of the displacements is a $[1\bar{1}0]$ direction. Thus the dislocation is of the "shuffle" type, as contrasted with the "glide" type. Some investigators, for example, Alexander (8), do not consider it to be the type that moves during plastic flow. However, one-third as many chemical bonds cross a unit area of the shuffle plane as compared with the glide plane, so it seems likely that "shuffle" kinks move most readily. For a complete review of core structures, see Duesbery and Richardson (9). Oxygen precipitation may account for the dislocation "dissociations" observed by transmission electron microscopy.

Movement of the kink into, or out of, the plane of the figure decreases the overlap of the bonding sp^3 orbitals between a pair of atoms (Fig. 3). This is followed by the formation of an overlap between one of the atoms of the initial pair and a different atom to make a new bonding pair.

The essence of the present model for low kink mobility is that the symmetry of the molecular orbitals plays a role that is similar to its role in determining the rates of chemical reactions according to the Woodward-Hoffmann theory (3). Movement of a kink is then akin to a chemical reaction in which an embedded "molecule" is dissociated, and then one of the product atoms joins with an atom from another dissociation to form a new "molecule." That is, kink movement is analogous to a simple substitution reaction such as the H-D reaction:

$$H' + HD \rightarrow H'D + H \qquad (1)$$

There are, of course, some important differences. In the case of the kink, the reaction coordinate is not simply a line along which displacements occur. Instead, it is a surface [a (111) plane of the diamond framework] along which shear strains occur (Fig. 3) in a $(1\bar{1}0)$ direction. Furthermore, at a kink the surface does not lie in a simply connected space; that is, a circuit taken around the dislocation kink does not close. The closure mismatch for one circuit is the Burgers vector, b. For n circuits, it is nb.

If the atoms on the top of the glide plane are labeled T and those on the bottom B, the reaction when the kink moves one step forward can be written:

$$B_1T + B_2 \rightarrow (B_1TB_2)^* \rightarrow B_1 + TB_2 \quad (2)$$

Here T slides over B_1 to form the transition complex, $(B_1TB_2)^*$, which then shears until T has its new partner, B_2. During this reaction the shear strain energy (which is proportional to the square of the shear strain) starts low, rises to a maximum, and then declines to zero. If the forces that arise during this process are defined by continuous potentials, the net resistance to the movement of the kink is relatively small (see Fig. 4) because, in this case, the variation of the energy with position is relatively small and smooth. Accordingly, the force tending to move the kink toward, or away from, the $x = w/2$ position would pass through zero at this position and would rise to a maximum at a position on one side or the other of the symmetric position. This has, in the past, led to the idea that kink mobility is high and therefore is not the rate-determining step for dislocation velocities in such a structure.

Following Burdett and Price (*10*), a correlation (Walsh) diagram for the "chemical reaction" just outlined is drawn in Fig. 4A. This shows graphically that the reaction is "disconcerted" in the Woodward-Hoffmann sense and therefore thermally forbidden. The diagram also indicates how to estimate the maximum force that is resisting kink motion and to calculate the pertinent activation energies.

The position within the kink is taken as the reaction coordinate. It varies from 0 to w. Initially the pertinent energy levels are ϵ_b (the HOMO, or top of the valence band, level) and ϵ_a (the LUMO, or bottom of the conduction band, level). Finally, after the kink has moved one position, the levels are the same. This is not a concerted reaction because bending of the sp^3 bonds causes the bonding levels to rise and the antibonding levels to fall as the reaction proceeds toward the transition state at $x = w/2$ (*11*). The reverse process occurs as the reaction recedes from the transition state. Therefore, the correlation lines cross at $x = w/2$, and the reaction is forbidden. More detailed considerations would show the existence of a gap at the crossing point, thereby removing the singularity, but this is not essential to the present discussion.

Figure 4A indicates that the maximum force on the kink lies at the $x = w/2$ position and also shows the difference between what is estimated from a classical Peierls-Nabarro potential and what is expected by looking at the behavior in terms of a quantum chemical reaction. It can be readily seen that the features of the correlation diagram have considerable consequences. Because of the broken symmetry of the molecular orbitals at the center of the kink, the energy has a sharp break at $x = w/2$, so the force $(\partial\epsilon/\partial x)$ becomes large (+ or −) and discontinuous there. However, the energy and forces remain finite.

The maximum force, $\partial\epsilon/\partial x$ at $x = w/2$, is sketched in the drawing for the parabolic energy dependencies expected for bond-bending (Fig. 4A). It equals $2(\Delta\epsilon/b)$ if we let $w = b$. Then, if the area on which the maximum force acts is taken to be $b^2/2$, the resistive stress is approximately $4(\Delta\epsilon/b^3)$. For silicon, $\Delta\epsilon = 1.2$ eV and $b = 3.76$ Å so the maximum stress is about 14.4 GPa (1440 kg/mm^2), which is comparable to observations.

The Walsh diagram also allows us to estimate the activation energy for dislocation motion. For this process, kinks must be both formed and moved. Thus, the overall activation energy is the sum of the formation and motion energies. Forming a pair of kinks means that two of them must be moved apart by at least one atomic distance, which takes an amount of energy, $E_{h\ell}$ = LUMO-HOMO gap. Moving one kink takes $E_{h\ell}/2$, but two kinks must be moved for net dislocation motion, which takes $E_{h\ell}$. Therefore, the overall activation energy is $2E_{h\ell}$, which is consistent with the data of Fig. 1.

It is interesting that what has been called hardness for centuries in the physical sciences is now directly linked through $E_{h\ell}$ to what chemists have begun, in recent decades, to call "hardness" (*12*). At high temperatures, the barrier to dislocation motion is the activation energy discussed above. This activation energy determines the hardness as shown in Fig. 5 (*13*). At

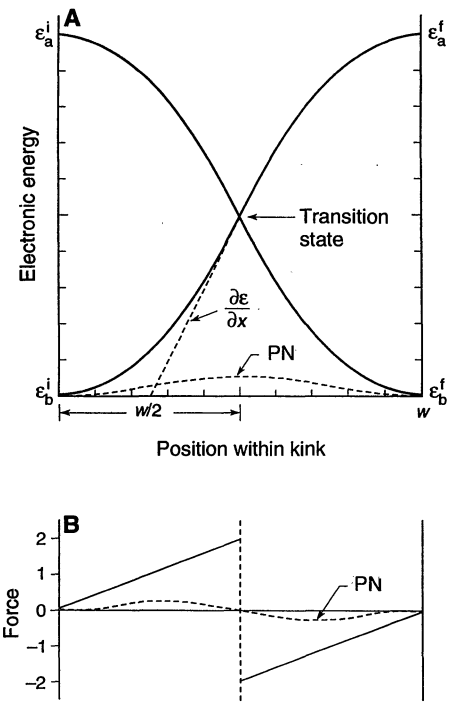

Fig. 4. (**A**) Correlation (Walsh) diagram for kink motion. The width of the kink is w, and the reaction coordinate is x; PN, Peierls-Nabarro theory. Bond bending causes the initial bonding energy level (ϵ_b^i) to rise with x^2 up to the transition state. It also causes the final antibonding level (ϵ_a^f) to decrease to the level of the transition state. Similarly, the initial antibonding level (ϵ_a^i) falls to the transition state level, and the final bonding level (ϵ_b^f) rises to the transition state. At the transition-state singularity, a small gap opens (not shown). The LUMO-HOMO gap vanishes at the transition state so the unpaired electron delocalizes. (**B**) The corresponding force diagram.

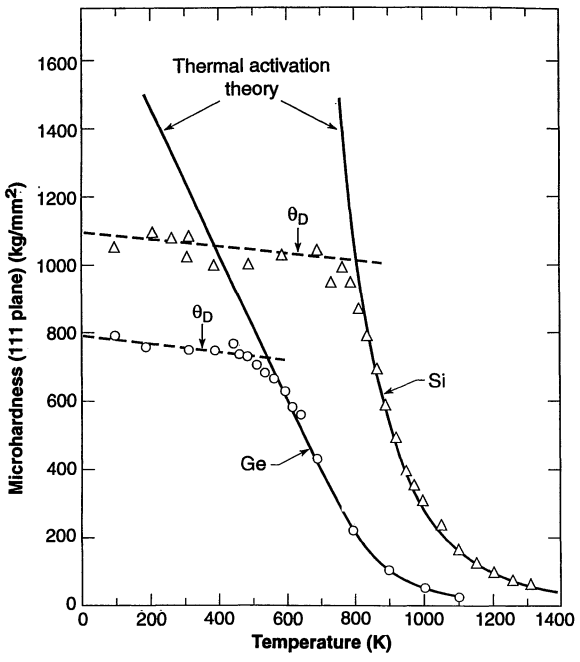

Fig. 5. Temperature dependence of the hardnesses of germanium and silicon. Data are from (*13*). Above the Debye temperatures, θ_D, where the thermal vibrations become intense, the hardness is determined by dislocation motion. Below θ_D, the hardness is determined by the critical compressive stress for transformation from the diamond to the β-tin structure.

low temperatures, two cases arise depending on whether the stress is compressive or tensile. In tension, the mobility is expected to decrease with decreasing temperature and the flow stress is expected to continue to rise along the thermal activation curves until fracture intervenes. In compression (including indentation hardness), shear-induced transformation to a metallic β-tin phase is encountered (*13*) and the indentation hardness becomes nearly independent of temperature as a result of the change in mechanism (*11*). (Because of its technical importance, silicon was chosen as the prototype for this discussion, but quite similar arguments apply to other covalent crystals, both pure and impure.)

Some secondary effects in the motion of dislocations in covalently bonded crystals include doping, polarity in compounds composed of elements from groups III and V, and photoplasticity. In the context of the present model, doping simply changes the HOMO-LUMO gap in the vicinity of the dopant atoms. The polarity effect (difference in mobility of dislocations with half-planes ending on anions versus those with half-planes ending on cations) is related to the piezoelectric effect in these noncentrosymmetric crystals. This creates local electric fields, which alter the HOMO and LUMO energy levels. In the photoplastic effect, electrons are excited across the HOMO-LUMO gap by incident photons, thereby obviating the need for thermal excitation.

REFERENCES AND NOTES

1. F. R. N. Nabarro, *Theory of Crystal Dislocations* (Dover, New York, 1987), p. 137.
2. J. P. Hirth and J. Lothe, *The Theory of Dislocations* (McGraw-Hill, New York, 1968), chap. 15.
3. R. B. Woodward and R. Hoffmann, *The Conservation of Orbital Symmetry* (Springer-Verlag, Weinheim, Germany, 1970).
4. H. Alexander and P. Haasen, *Solid State Phys.* **22**, 28 (1968).
5. K. Sumino, *Inst. Phys. Conf. Ser.* **104**, 245 (1989).
6. J. J. Gilman, *J. Appl. Phys.* **46**, 5110 (1975).
7. J. C. Phillips, *Bonds and Bands in Semiconductors* (Academic Press, New York, 1973), chap. 3.
8. H. Alexander, *J. Phys. (Paris) Colloq.* **40**, C6-1 (1979).
9. M. S. Duesbery and G. Y. Richardson, *Solid State and Material Sciences* (CRC Press, Boca Raton, FL, 1991), vol. 17, p. 1.
10. J. K. Burdett and S. L. Price, *Phys. Rev. B* **25**, 5778 (1982).
11. J. J. Gilman, *Philos. Mag. B* **67**, 207 (1993).
12. Z. Zhou and R. G. Parr, *Tetrahedron Lett.* **29**, 4843 (1988). See also P. W. Atkins, *Quanta* (Oxford Univ. Press, Oxford, 1991), p. 151.
13. V. I. Trefilov and Yu. V. Mil'man, *Sov. Phys. Dokl.* **8**, 1240 (1964).

14. This work was supported by the Director, Office of Energy Research, Office of Basic Energy Sciences, Materials Sciences Division, U.S. Department of Energy under contract DE-AC03-76F00098.

26 April 1993; accepted 24 June 1993

Convergent Regulation of Sodium Channels by Protein Kinase C and cAMP-Dependent Protein Kinase

Ming Li, James W. West, Randal Numann, Brian J. Murphy, Todd Scheuer, William A. Catterall

The function of voltage-gated sodium channels that are responsible for action potential generation in mammalian brain neurons is modulated by phosphorylation by adenosine 3′,5′-monophosphate (cAMP)–dependent protein kinase (cA-PK) and by protein kinase C (PKC). Reduction of peak sodium currents by cA-PK in intact cells required concurrent activation of PKC and was prevented by blocking phosphorylation of serine 1506, a site in the inactivation gate of the channel that is phosphorylated by PKC but not by cA-PK. Replacement of serine 1506 with negatively charged amino acids mimicked the effect of phosphorylation. Conversion of the consensus sequence surrounding serine 1506 to one more favorable for cA-PK enhanced modulation of sodium currents by cA-PK. Convergent modulation of sodium channels required phosphorylation of serine 1506 by PKC accompanied by phosphorylation of additional sites by cA-PK. This regulatory mechanism may serve to integrate neuronal signals mediated through these parallel signaling pathways.

Action potentials in neurons are initiated by the opening of voltage-gated Na^+ channels. Although the rat brain Na^+ channel is a heterotrimer that consists of an α subunit of 260 kD, a β_1 subunit of 36 kD, and a β_2 subunit of 33 kD (*1*), the α subunit alone is sufficient to form functional voltage-gated ion channels when expressed from cloned complementary DNA in *Xenopus* oocytes (*2*) or mammalian cells (*3*, *4*). Alpha subunits of rat brain Na^+ channels are phosphorylated by cA-PK (*5*) and PKC (*6*), and four α subunits have been cloned and sequenced from rat brain (*7*, *8*). The large intracellular loop between homologous domains I and II ($L_{I/II}$) in each of these Na^+ channels contains multiple consensus sites (*9*) for phosphorylation by cA-PK and PKC that are phosphorylated in vitro and in intact cells (*10*, *11*).

Phosphorylation of rat brain Na^+ channels by PKC at Ser^{1506} in the inactivation gate formed by the short intracellular loop between domains III and IV ($L_{III/IV}$) slows their inactivation (*12*, *13*), and subsequent phosphorylation by PKC of a site in $L_{I/II}$ reduces peak Na^+ currents (*14*). Phosphorylation of Na^+ channels by cA-PK in $L_{I/II}$ also reduces the peak Na^+ current in excised membrane patches from cultured rat brain neurons, transfected mammalian cells, and *Xenopus* oocytes that express brain Na^+ channels (*15*, *16*). The reduction in peak current is caused by failure of channel activation during depolarizing stimuli, but the time course of Na^+ channel inactivation is not noticeably affected (*15*). Here, we show that phosphorylation of Na^+ channels through these two signaling pathways interacts to cause convergent regulation of Na^+ channel function.

Because peak Na^+ currents in excised membrane patches are reduced by treatment with cA-PK (*15*), we were surprised to observe that treatment of intact Chinese hamster ovary (CHO) cells that stably express rat brain type IIA Na^+ channel α subunits (CNaIIA-1 cells) (*4*) with the membrane-permeant analog 8-bromo–adenosine 3′,5′-monophosphate (8-Br-cAMP) either had no effect on peak Na^+ currents or increased peak Na^+ currents (Fig. 1A) recorded in cell-attached membrane patches (*17*). Because both cA-PK and PKC reduce peak Na^+ current in excised patches, we examined the interaction between these two kinases in modulating rat brain Na^+ channel function in intact cells. Partial activation of PKC by treatment with an intermediate concentration (25 μM) of oleoylacetylglycerol (OAG) slowed the inactivation of the Na^+ current in cell-attached patches but did not reduce the peak Na^+ current (Fig. 1, B and C) (*14*). Subsequent addition of 8-Br-cAMP in the presence of OAG reduced peak Na^+ current, which indicates that PKC phosphorylation was required to observe an effect of phosphorylation by cA-PK (Fig. 1, B and C).

To examine the mechanism of this regulatory interaction, we studied the effects of cA-PK on Na^+ currents in excised inside-out patches (*17*) from CHO cells that expressed either wild-type or mutant Na^+ channels in which Ser^{1506}, the site of phos-

Department of Pharmacology, SJ-30, University of Washington, Seattle, WA 98195.